Noise-induced excitation wave and its size distribution in coupled FitzHugh-Nagumo equations on a square lattice

Hidetsugu Sakaguchi
Interdisciplinary Graduate School of Engineering Sciences, Kyushu University, Kasuga, Fukuoka 816-8580, Japan

(Received 10 January 2024; accepted 22 March 2024; published 19 April 2024)

There are various research topics such as stochastic resonance, coherent resonance, and neuroavalanche in excitable systems under external noises. We perform numerical simulation of coupled noisy FitzHugh-Nagumo equations on the square lattice. Excitation waves are generated most efficiently at an intermediate noise strength. The cluster size distributions obey a power-law-like distribution at a certain parameter range. However, we consider that this is not a self-organized critical phenomenon, partly because the exponent of the power law is not constant. We have studied the propagation of excitation waves in the coupled noisy FitzHugh-Nagumo equations with a one-dimensional pacemaker region and found that there is a phase-transition-like phenomenon from the short-range propagation to the whole-system propagation by changing the noise strength T. The power-law distribution is observed most clearly near the phase transition of the propagation of excitation waves in the coupled noisy FitzHugh-Nagumo equations without the one-dimensional pacemaker.

DOI: 10.1103/PhysRevE.109.044211

I. INTRODUCTION

Neural networks are composed of a lot of neurons. If there is no external input, the neuron is in a stationary state; however, it is excited and emits a spiking output if the input is beyond a threshold. From the viewpoint of nonlinear dynamics, the neuron is an excitable system. The Hodgkin-Huxley equation is a typical nonlinear equation that describes the spiking of a giant axon of squid [1]. The FitzHugh-Nagumo equation is a simple model equation that exhibits a similar spiking phenomenon [2,3]. Various nonlinear phenomena such as chaos and the suppression of spiking by high-frequency stimulation were studied by many authors [4–6]. Noise effects for excitable systems were also studied by many authors [7,8]. Rather coherent oscillation induced by noise is called coherence resonance [9]. The response is maximized at a suitable noise strength, if a periodic driving force is added to the noisy excitable systems. It is called stochastic resonance, which was originally found in bistable systems [10]. In globally coupled noisy excitable systems, there is a phase transition from the stationary state to the oscillatory state [11–13]. Coherent resonance was also studied in one- and two-dimensional arrays of nonidentical excitable units with a strong coupling constant driven by additive noises, in which phase coherence was observed at intermediate noise strength [14]. Noise-induced wave propagations were studied in one- and two-dimensional excitable systems [15,16]. Power-law distributions of spatiotemporal clusters were reported in some noise-driven excitable systems [17,18]. The avalanches of neural activities and the power-law distributions were reported in slices of rat cortex [19]. The exponent of the power law was evaluated as -1.5. Furthermore, a power law was reported in the electrical activity in human electroencephalography [20]. Several authors consider that the power-law distributions are related to the self-organized criticality. Various theoretical models have been proposed for the self-organized criticality [21–24].

In this paper, we numerically study the noise-induced excitation waves in coupled noisy FitzHugh-Nagumo equations. The nucleation of excitation waves and their propagation are reproduced in our system. We use a type of local order parameter to reduce the fluctuations. We find a power-law-like distribution for the spatiotemporal clusters of the local order parameter in a certain parameter range. We further study the wave propagation sent out from a linear pacemaker region; and find a transition from the short-range propagation to the long-range propagation. Near the critical line of the phase transition, the power-law distributions appear most clearly. We consider that the power-law behavior is related to the phase transition of the stochastic propagation of excitation waves.

II. COUPLED NOISY FITZHUGH-NAGUMO EQUATIONS ON A SQUARE LATTICE

We study a two-dimensional system on a square lattice expressed as

$$\begin{aligned}\frac{du_{i,j}}{dt} &= u_{i,j}(u_{i,j}+a)(1-u_{i,j}) - v_{i,j} + I \\ &\quad + K\sum_j (u_{i+1,j}+u_{i-1,j}+u_{i,j+1}+u_{i,j-1}-4u_{i,j}) \\ &\quad + \xi_{i,j}(t), \\ \frac{dv_{i,j}}{dt} &= \epsilon(u_{i,j}-bv_{i,j}), \\ &\quad i=1,2,\ldots,L,\ \ j=1,2,\ldots,L, \end{aligned} \tag{1}$$

where K is the coupling constant and set to be 0.5 in this paper. The other parameters a, b, and ϵ are set to $a = 0.02$,

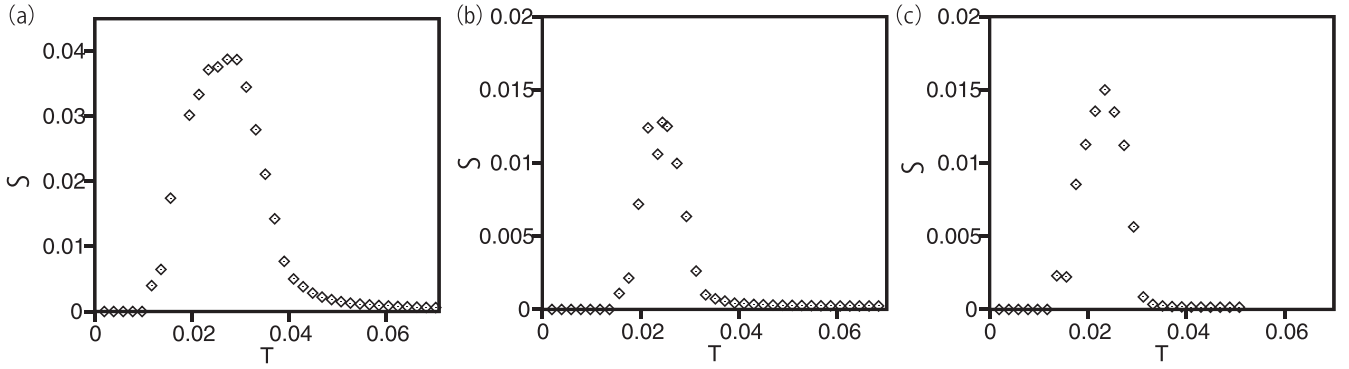

FIG. 1. (a) Order parameter S as a function of T at $I = -0.135$ in a system of $L \times L = 100 \times 100$. (b) S as a function of T at $I = -0.15$ in a system of 100×100. (c) S as a function of T at $I = -0.15$ in a system of 200×200.

$b = 1$, and $\epsilon = 0.002$. I is the input to the system, and $\xi_{i,j}$ denotes the Gaussian white noise satisfying $\langle \xi_{i,j}(t)\xi_{i',j'}(t')\rangle = 2T\delta_{i,i'}\delta_{j,j'}\delta(t-t')$. In case of $T = 0$, each elemental system is oscillatory for $I > -0.00872$, but it becomes excitable for $I < -0.00872$ [6]. In the excitable system, u takes a resting state if there are no additional external input and noise. For a sufficiently small $|I|$, u takes a constant value $u_s \simeq I/(1-a)$ at the resting state. When each element is excited, u goes to around one. We call each element at the (i, j) site excited if $u_{i,j}$ goes over a criterion value $u_c = 0.5$, since 0.5 is close to an average value of the stationary value $I/(1-a)$ and the peak value around one. We define a local order parameter $s_{i,j}$ as $s_{i,j}$ takes one only if $u_{i,j} > 0.5$, $u_{i+1,j} > 0.5$, $u_{i-1,j} > 0.5$, $u_{i,j+1} > 0.5$, $u_{i,j-1} > 0.5$, and $s_{i,j} = 0$, if at least one of the five values of u is smaller than 0.5. The order parameter S is the average value of $s_{i,j}$, that is, $S = (1/L^2)\sum_{i,j} s_{i,j}$. If $u_{i,j} > 0.5$ for all i and j, the order parameter $S = 1$. Figures 1(a) and 1(b) are the temporal average of S as a function of T at (a) $I = -0.135$ and $I = -0.15$. The system size is $L \times L = 100 \times 100$. The no-flux boundary conditions are used at $i = 1$, $i = L$, $j = 1$, and $j = L$. Figure 1(c) is the temporal average of S as a function of T at $I = -0.15$ for the system size 200×200. A similar peak structure is observed even at the larger system. The order parameter takes a maximum at an intermediate range of noise strength. This is a kind of coherent resonance in coupled excitable systems. If we use another simpler local order parameter $s'_{i,j}$ where $s'_{i,j} = 1$ only if $u_{i,j} > 0.5$, a similar peak structure is observed for $S' = \sum_{i,j} s'_{i,j}$; however, S' does not take a one-hump structure but increases with T for larger T. Hereafter, we use the local order parameter $s_{i,j}$. The peak value of S is smaller and the width is narrower at $I = -0.15$ compared to the case of $I = -0.135$. Figure 2 shows a parameter range where the temporal average of S takes a value larger than 0.001 in the parameter space (T, I) calculated in a system of 100×100.

Figure 3 shows the spatiotemporal patterns of lattice points satisfying $u_{i,j} > 0.5$ at $j = L/2$, at (a) $T = 0.0254$, and (b) $T = 0.0390$ for $I = -0.135$. At $T = 0.0254$, a spot of excited sites appears by thermal noises, the excitation wave propagates to almost the entire system, and disappears at the boundaries. The nucleation occurs at any position, but the nucleation frequency is higher at the boundaries, especially at the four corners. Under the periodic boundary conditions, the nucleation probability is the same for the whole region, however, the nucleated one-dimensional waves do not disappear and continue to propagate if the noise strength is sufficiently weak. We therefore adopt the no-flux boundary conditions in this paper. At $T = 0.0390$, the generation of excitation waves occurs more frequently by the thermal noises, but the excitation waves disappear owing to the stronger noises before they reach the boundaries.

Figures 4(a), 4(b), and 4(c) show three snapshots of lattice points satisfying $u_{i,j} > 0.5$ at (a) $t = 5850$, (b) $t = 5855$, and (c) $t = 5870$ at $T = 0.0390$ for $I = -0.135$. An excited spot appears near $i = 62$ and $j = 90$ at $t = 5850$, and it expands in the surrounding. If there are no noises, a ringlike wave would propagate to the entire system. However, the ringlike wave breaks in pieces and disappears by the noises as shown in Fig. 4(c). The noises have an effect to break the excitation wave.

Figure 5(a) is the time evolution of S at $T = 0.0254$ for $I = -0.135$. The peak amplitudes have a similar magnitude because the noise-induced excitation propagates almost to the entire system as shown in Fig. 3(a). Figures 5(b) and 5(c) are time evolutions of S at (b) $T = 0.0352$ and (c)

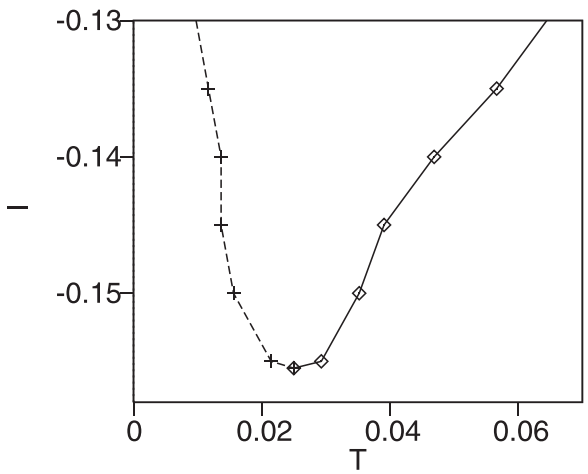

FIG. 2. Parameter range where the temporal average of S takes a value larger than 0.001 in the parameter space (T, I) calculated in a system of 100×100.

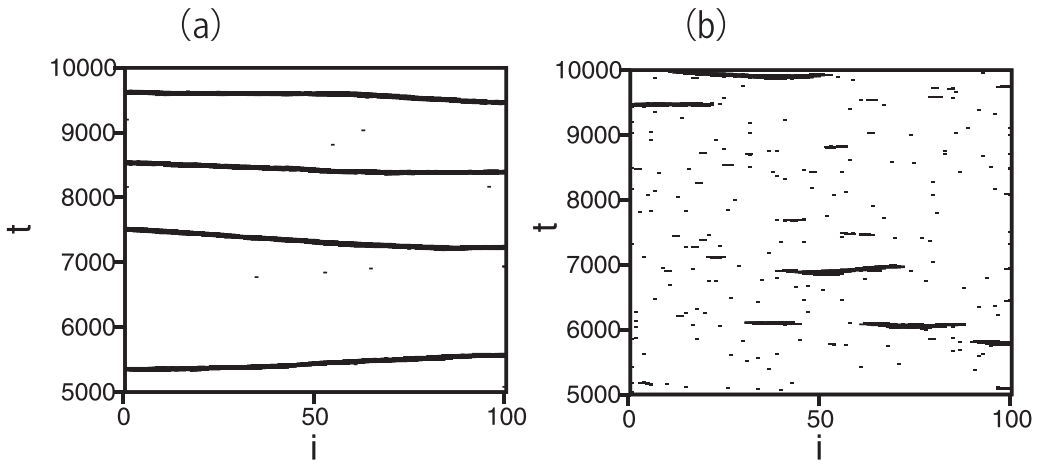

FIG. 3. Time evolutions of lattice points satisfying $u_{i,j} > 0.5$ at $j = L/2$, at (a) $T = 0.0254$, and (b) $T = 0.0390$ for $I = -0.135$. At the black dot positions, $u_{i,j}$ takes a value larger than 0.5.

$T = 0.0547$ for $I = -0.15$. Intermittent time evolutions are observed at $T = 0.0352$ and 0.0547. The peak amplitudes become smaller with T. Figures 6(a) and 6(b) show the probability distributions of the cluster size C at $T = 0.0371$ and $I = -0.15$ for system size (a) $L \times L = 100 \times 100$ and (b) 200×200 at $T = 0.0371$ in a double-logarithmic scale. Here, spatiotemporal clusters are constructed using the local order parameter $s_{i,j,n}$ observed at discrete times $t = 5n$ (n is an integer). [The velocity of a single pulse is around 0.2 and the width is around ten as shown later in Fig. 9(a) when the noise is absent. The time interval $\Delta t = 5$ is a time scale for the single pulse to propagate by one lattice interval]. That is, the site (i, j, n) on the three-dimensional lattice and the neighboring site (i', j', n') of the (i, j, n) site are connected if $s_{i,j,n} = 1$ and $s_{i',j',n'} = 1$. A spatiotemporal cluster is defined as a set of locally connected lattice points. The cluster size C is defined as the total number of lattice points included in one cluster. The two probability distributions for 100×100 and 200×200 have a similar form. The probability distribution can be approximated at a power-law distribution, although it is slightly curved downward. Figure 6(c) shows the cluster size distribution in which $s'_{i,j}$ is used for the local order parameter instead of $s_{i,j}$ to investigate the influence on the choice of the local order parameter. If the local order parameter s' is used, many small clusters of excited sites of $s' = 1$ are generated and the probability distribution takes a higher value for small C. However, the probability distribution can be approximated at a power-law distribution for $C > 10$. We consider that the probability distribution does not depend on the choice of the local order parameter for large C. Hereafter, we use $s_{i,j}$ to calculate the probability distribution.

Figure 7(a) shows the cumulative distributions $Q(C) = \int_C^\infty P(C')dC'$ of the cluster size at $T = 0.0254$, 0.0371, and 0.0742 for $I = -0.15$. The power-law behavior is seen in a finite range of T at the three parameter values but the exponent is different for the three parameters. For example, a power-law-like behavior of exponent 1.20 ± 0.002 is seen for $20 < C < 10\,000$ at $T = 0.0254$. The exponent is evaluated as 1.71 ± 0.006 for $50 < C < 500$ at $T = 0.0371$, and 2.95 ± 0.04 for $5 < C < 50$ at $T = 0.0742$. We do not consider that this is a self-organized critical phenomenon partly because the exponent is not constant. The exponent is uniquely determined in most models of self-organized criticality, such as the sand-pile model by Bak, Tang, and Wiesenfeld [21] and the

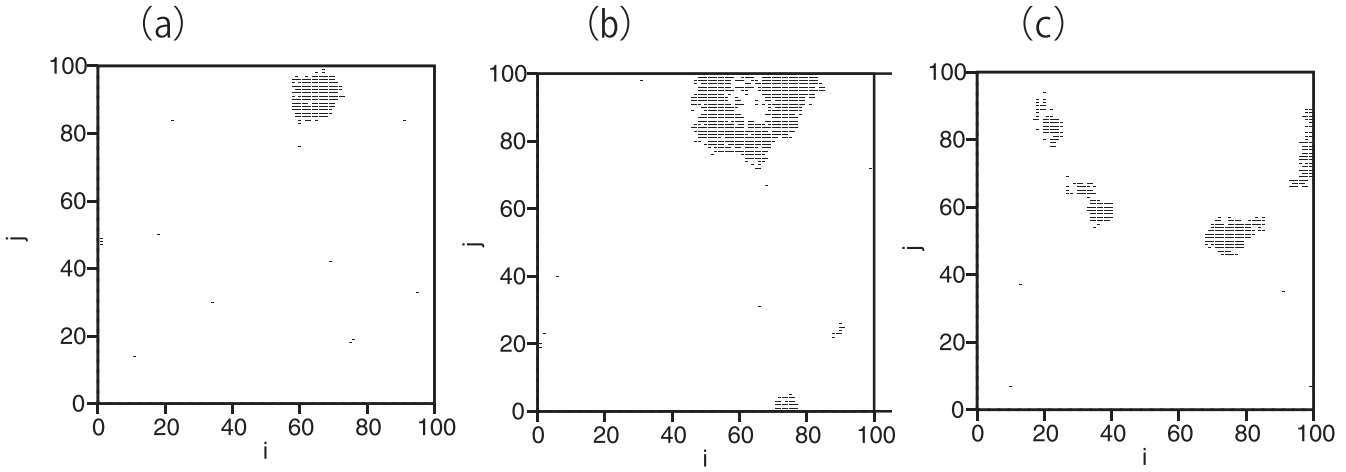

FIG. 4. Three snapshots of the regions of $u_{i,j} > 0.5$ at (a) $t = 5850$, (b) $t = 5855$, and (c) $t = 5870$ at $T = 0.0390$ for $I = -0.135$.

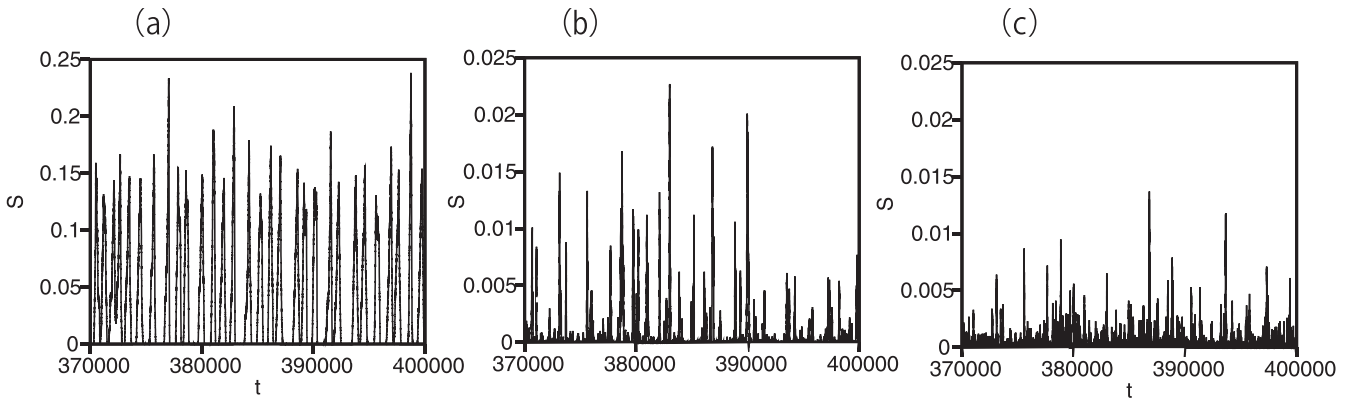

FIG. 5. Time evolutions of S at (a) $T = 0.0254$ and $I = -0.135$, (b) $T = 0.0352$ and $I = -0.15$, and (c) $T = 0.0547$ and $I = -0.15$.

self-organized depinning transition model [25,26], although there are some models such as the Olami-Feder-Christensen model [27] in which the exponent changes with the system parameter. The cumulative distribution is slightly curved upward for $1000 < C < 10\,000$ at $T = 0.0254$, which represents the excitation waves expanding to the entire system. At $T = 0.0742$, the cumulative distribution is curved downward, since the excitation waves decay quickly. At $T = 0.0371$, the cumulative distribution is slightly curved downward, although various sizes of excited waves appear at this parameter. Figure 7(b) shows the average cluster size $< C >$ as a function of T for $I = -0.15$. The average cluster size decreases with T because the excitation waves disappear more quickly for larger T.

III. WAVE PROPAGATION IN TWO-DIMENSIONAL COUPLED NOISY FITZHUGH-NAGUMO EQUATIONS WITH A ONE-DIMENSIONAL PACEMAKER

The dynamical behaviors of the two-dimensional coupled noisy FitzHugh-Nagumo equations are determined by the nucleation of excitation waves and their decay during propagation. Both the nucleation and decay are caused by the noise effects. The probability of the nucleation is expected to follow the Arrhenius law and the probability decreases rapidly as $\exp(-\Delta E/T)$ near $T = 0$, and there is no critical point. On the other hand, there is a possibility of phase transition for the propagation of excitation waves on the square lattice. That is, the excitation wave decays soon after the nucleation for large T, but the excitation waves survive long and reach the boundary below a critical value of T. On the one-dimensional lattice, the excitation wave disappears once the propagation is blocked at a lattice site by the noise, however, the excitation wave can propagate on the square lattice by the excitation from the neighboring sites even if the excitation wave is blocked at a site by the noise.

To make the transition clearer, a source region of excitation waves is set for $1 \leqslant j \leqslant 5$. That is, we use a modified model equation,

$$\begin{aligned}
\frac{du_{i,j}}{dt} &= u_{i,j}(u_{i,j}+a)(1-u_{i,j}) - v_{i,j} \\
&\quad + K\sum_{j}(u_{i+1,j}+u_{i-1,j}+u_{i,j+1}+u_{i.j-1}-4u_{i,j}) \\
&\quad + \xi_{i,j}(t) + I_{i,j}, \\
\frac{dv_{i,j}}{dt} &= \epsilon(u_{i,j} - bv_{i,j}), \\
i &= 1,2,\ldots,L_x \;\; j = 1,2,\ldots,L_y,
\end{aligned} \tag{2}$$

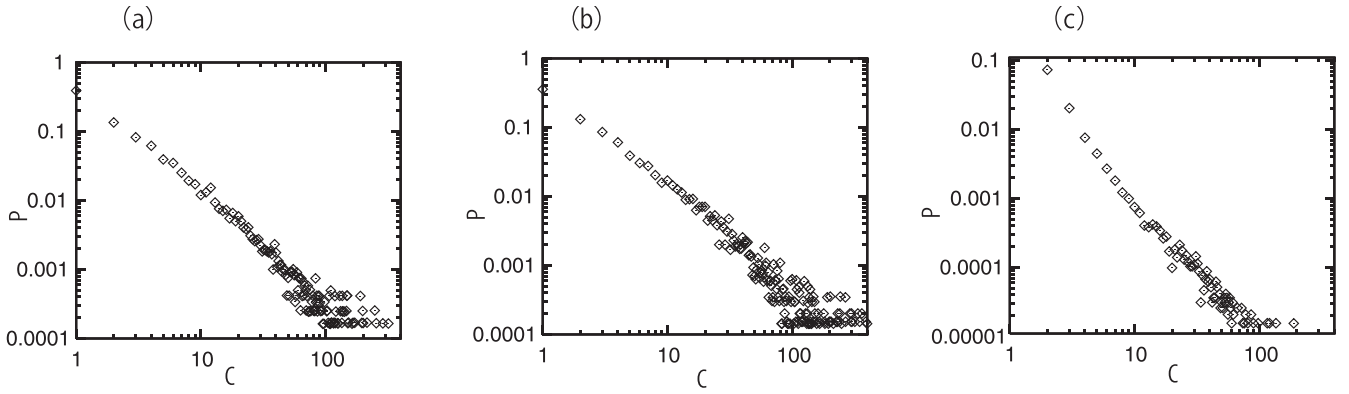

FIG. 6. Probability distribution of the cluster size C at $T = 0.0371$ and $I = -0.15$ for system size (a) $L \times L = 100 \times 100$ and (b) 200×200 at $T = 0.0371$ in a double-logarithmic scale. (c) Probability distribution of the cluster size C of s' at $T = 0.0371$ and $I = -0.15$ for system size $L \times L = 100 \times 100$.

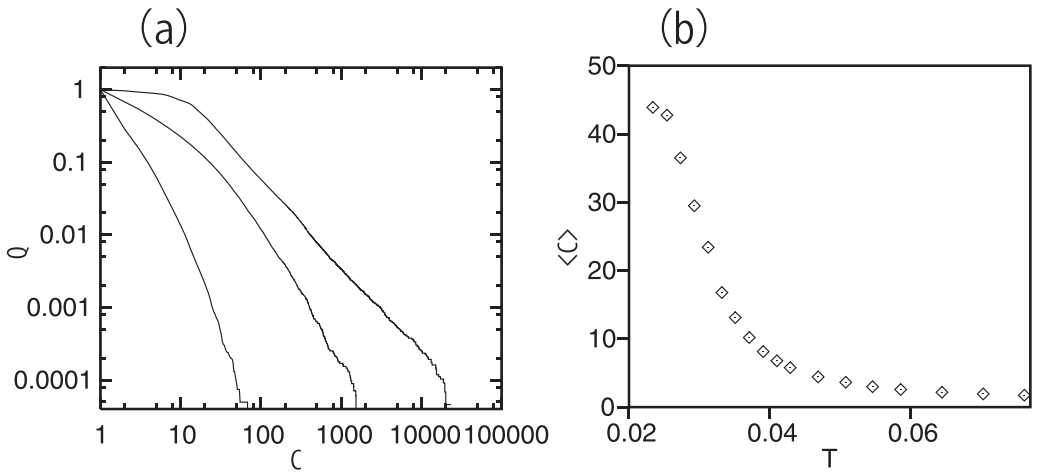

FIG. 7. (a) Cumulative distribution function $Q(C) = \int_C^\infty P(C')dC'$ of the cluster size C at $T = 0.0254$, 0.0371, and 0.0742 for $I = -0.15$. (b) Average cluster size $< C >$ as a function of T for $I = -0.15$.

where $I_{i,j} = I_0 = 0.015$ and $T_{i,j} = 0$ for $1 \leqslant j \leqslant 5$ and $I_{i,j} = I$, and $T_{i,j} = T$ for the other lattice points. The system size is assumed to be $L_x \times L_y = 50 \times 300$. The periodic boundary conditions are adopted at $i = 1$ and $i = L_x$. The excitation waves are periodically generated from the pacemaker region and the propagation dynamics of the excitation waves can be observed clearly. In other words, we don't need to consider the nucleation process of the excitation waves. Figure 8 shows the five snapshots of lattice points of $s_{i,j} = 1$ at $t = 6000$, 6200, 6400, 6600, and 6800 at $I = -0.15$ and $T = 0.0293$. Excitation waves are generated at $1 \leqslant j \leqslant 5$ and propagate toward $j = L_y$. One-dimensional excitation waves propagate in the y direction. The excitation waves fluctuate, break up, and decay owing to the noise effect. The excitation wave in Fig. 8 disappeared near $j = 220$ at $t = 7200$. Figures 9(a), (b), and (c) plot the lattice point j where $s_{i,j}$ takes one at least at one lattice point (i, j) at (a) $T = 0.0215$, (b) $T = 0.0293$, and (c) $T = 0.0371$ for $I = -0.15$. At $T = 0.0215$, all the excitation waves propagate in the j direction and reach the boundary $j = L_y$. At $T = 0.0371$, the excitation waves propagate in the j direction but decay at $20 < j < 60$. At $T = 0.0293$, the propagation length changes for each period. There is a phase transition from the short-range propagation to the whole-system propagation by changing the noise strength T. The transition is analogous to the directed percolation [28]. There is a phase transition from a nonpercolating state to a percolating state in the directed percolation. In the percolating state, there is an infinitely large mutually connected spatio-temporal cluster. The essential difference from the directed percolation is that there is no absorbing state in our system. Figure 10(a) shows the average value of j for the lattice points satisfying $s_{i,j} = 1$ as a function of T for $I = -0.15$. The average value takes a value close to $L_y/2$ for sufficiently small T because all lattice points are excited. The average value decreases rapidly near $T = 0.03$. We evaluated the critical value as $T_c = 0.0298$ for $I = -0.15$, in that only one excitation wave reaches $j = L_y$ for $0 < t < 20\,000$. The critical value T_c increases with I. Figure 10(b) shows the critical values T_c for several I's in the parameter space of T and I. The critical line is located inside the parameter range of noised-induced wave propagation shown in Fig. 2. On the left of the critical line, the nucleation of excitation waves is rare, however, the excitation waves survive for a long time. On the right of the critical line, excitation waves are frequently generated, however, the excitation waves decay quickly. Near the critical line, various sizes of excitation waves are generated, and the size distribution is expected to obey a power law more clearly.

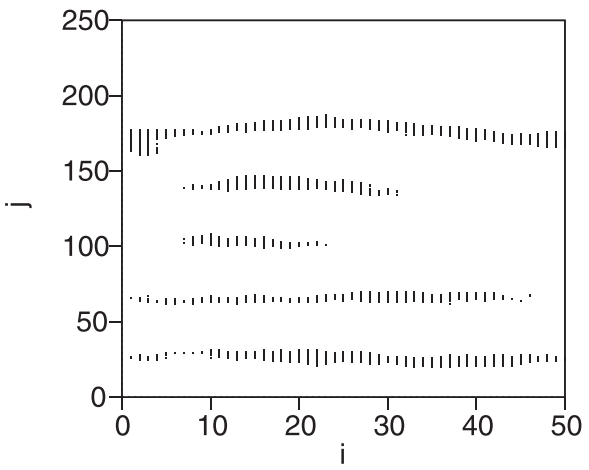

FIG. 8. Propagation of excitation waves at $I = -0.15$ for $T = 0.0293$ by Eq. (2). Five snapshots of lattice points satisfying $s_{i,j} = 1$ at $t = 6000$, 6200, 6400, 6600, and 6800 are plotted.

IV. CRITICAL STATES AND THE FEEDBACK CONTROL OF THE CRITICAL STATES

We have performed numerical simulations of Eq. (1) again near the critical line of the propagation of excitation waves. Figures 11(a) and 11(b) show the size distributions at (a) $T = 0.0298$ and $I = -0.15$, and (b) $T = 0.0342$ and $I = -0.14$. A power-law-like behavior is observed for $S > 30$. The exponent is approximated by the least-square method at 2.13 ± 0.02 for $T = 0.0298$ and $I = -0.15$, and 2.15 ± 0.02 for $T = 0.0345$ and $I = -0.14$. Figure 11(c) shows the size distribution for a larger system of 300×300 at $T = 0.0298$ and $I = -0.15$. The exponent is evaluated as 1.85 ± 0.04,

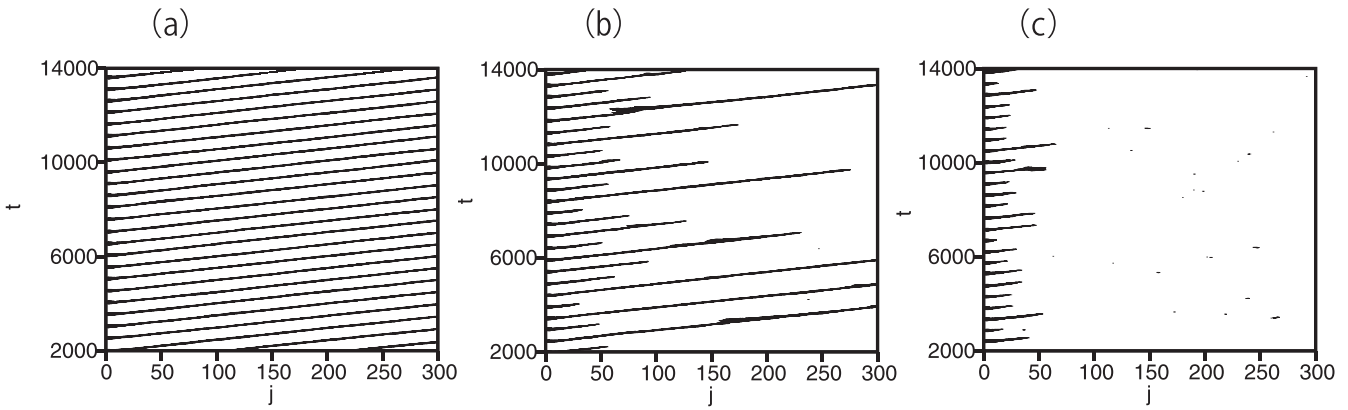

FIG. 9. Propagation of excitation waves at (a) $T = 0.0215$, (b) $T = 0.0293$, and (c) $T = 0.0371$ for $I = -0.15$. The j coordinate of the excited lattice points (i, j) is plotted at time $t = 5n$ (n: integer).

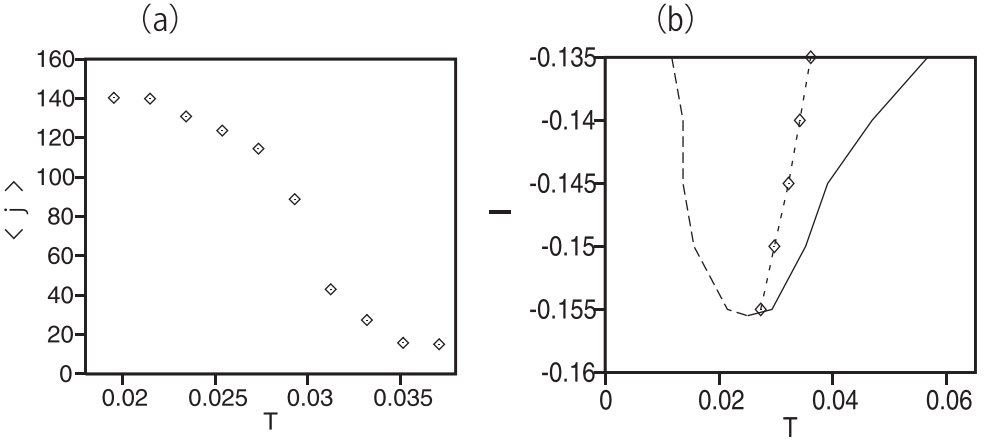

FIG. 10. (a) Average value of j for the lattice points satisfying $s_{i,j} = 1$ as a function of T for $I = -0.15$. (b) The critical line of the propagation of the excited wave in the parameter space of (T, I).

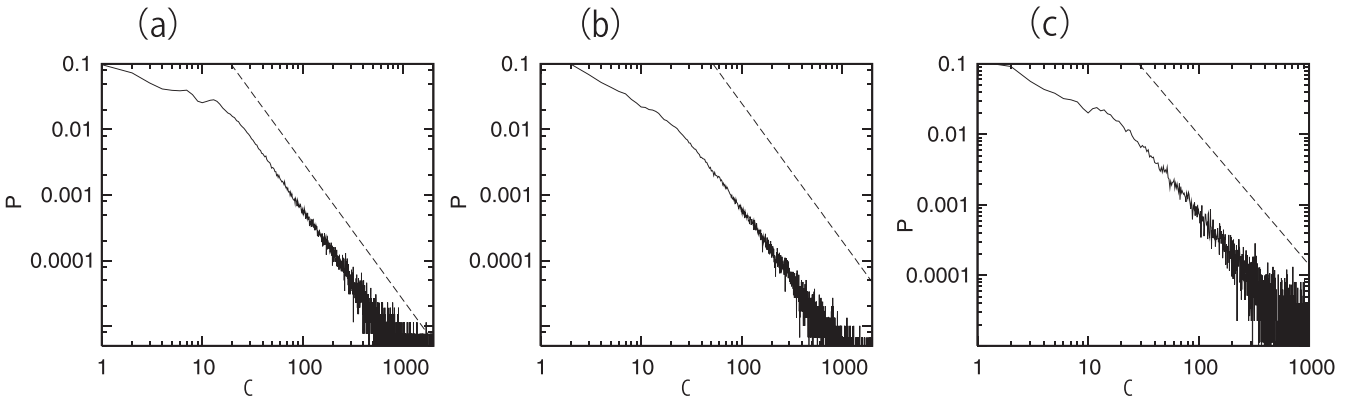

FIG. 11. Cluster size distributions at (a) $T = 0.0298$, $I = -0.15$ and (b) $T = 0.0342$, $I = -0.14$. The dashed lines denote the power law of exponent -2.1. (c) Cluster size distributions at (a) $T = 0.0298$, $I = -0.15$ in a larger system of 300×300. The dashed line denotes the power law of exponent -1.85.

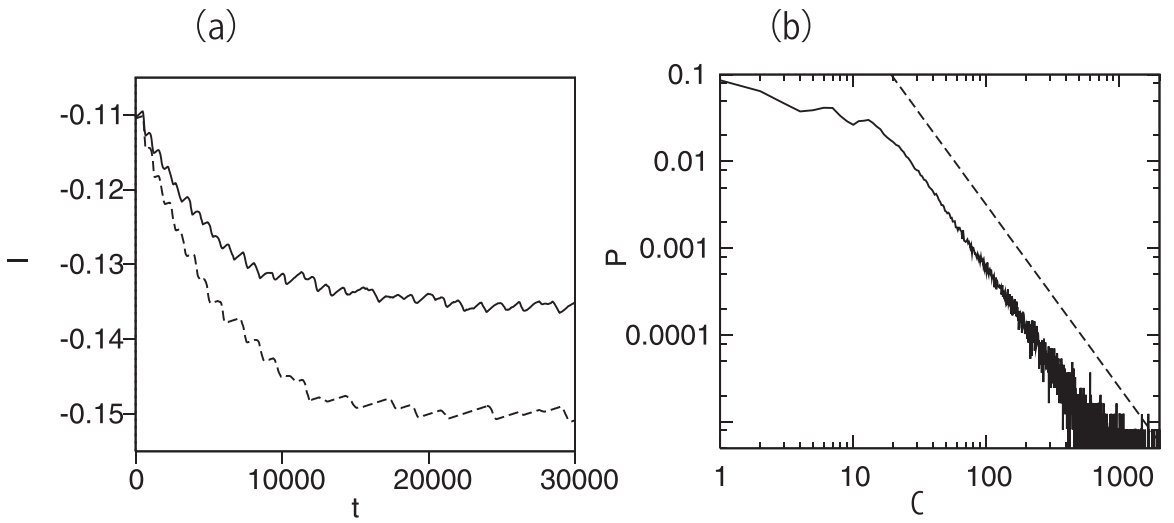

FIG. 12. (a) Time evolutions of $I(t)$ by Eq. (3) at $T = 0.0361$, $S_0 = 0.01767$ (solid line) and $T = 0.0293$, $S_0 = 0.00635$ (dashed line) for $\epsilon' = 0.0001$. (b) Cluster size distribution at $T = 0.0293$, $S_0 = 0.00635$, and $\epsilon' = 0.0001$. The dashed lines denote the power law of exponent -2.1.

although the temporal range is smaller by 1/5 than the case of system size 100×100 owing to the limit of memory. In an even larger system of 500×500, the exponent could not be evaluated because of the lack of memory to store the spatiotemporal cluster. The precise evaluation of the exponent is left to future study.

Finally, we show a few numerical simulations to obtain the critical state by the feedback control. The model equation is

$$\begin{aligned}
\frac{du_{i,j}}{dt} &= u_{i,j}(u_{i,j}+a)(1-u_{i,j}) - v_{i,j} \\
&\quad + K\sum_j (u_{i+1,j}+u_{i-1,j}+u_{i,j+1}+u_{i.j-1}-4u_{i,j}) \\
&\quad + \xi_{i,j}(t) + I(t), \\
\frac{dv_{i,j}}{dt} &= \epsilon(u_{i,j} - bv_{i,j}), \\
i &= 1,2,\ldots L, \quad j = 1,2,\ldots,L, \\
\frac{dI}{dt} &= \epsilon'(S_0 - S(t)),
\end{aligned} \tag{3}$$

where S_0 is the target value of the order parameter S. In this model, the input $I(t)$ is controlled by the feedback term as the order parameter is close to the target value S_0.

Figure 12(a) shows the time evolutions of $I(t)$ at $T = 0.0361$, $S_0 = 0.01767$ (solid line), and $T = 0.0293$, $S_0 = 0.00635$ (dashed line) for $\epsilon' = 0.0001$. The system size is 100×100. The parameters S_0's were chosen as $S_0 = 0.02767$ for $T = 0.0361$ and $S_0 = 0.01767$ for $T = 0.0293$, which are the values of the order parameter S shown in Figs. 1(a) and 1(b) at the critical parameters I_c shown in Fig. 10(b) for the two values of T. The initial value of $I(t)$ is $I(0) = -0.11$. Figure 12(a) shows that $I(t)$ is fluctuating near the critical value I_c after an initial transient time. Figure 12(b) shows the cluster size distribution in a double-logarithmic scale obtained by Eq. (3) for $30\,000 < t < 150\,000$ at $T = 0.0293$, $S_0 = 0.00635$, and $\epsilon' = 0.0001$. The exponent of the power-law fitting is 2.13 ± 0.025. A nearly critical state is realized by Eq. (3) owing to the feedback control. There are various theories that the brains are working near a critical state [19,22,24,29,30]. Our model equation is a quite simple one, but there is a possibility that the nearly critical state is realized by some feedback control methods. We would like to investigate a more plausible feedback model in the future.

V. SUMMARY

We have performed a numerical simulation of coupled noisy FitzHugh-Nagumo equations on a square lattice. We have confirmed that excitation waves are generated most efficiently at an intermediate range of noise strength. The cluster size distributions obey a power-law-like distribution at a certain parameter range. However, we consider that this is not a self-organized critical phenomenon, partly because the exponent of the power law is not constant. We have studied the propagation of the excitation waves in the coupled noisy FitzHugh-Nagumo equations with a one-dimensional pacemaker region. We have found that there is a transition from the short-range propagation to the whole-system propagation by changing the noise strength T. This phase-transition-like phenomenon is the main finding of this paper. We have checked that the power-law distribution is observed most clearly near the phase transition points of the propagation of excitation waves in the coupled noisy FitzHugh-Nagumo equations without the one-dimensional pacemaker. We interpret that the power-law-like behavior is related to this phase transition of the stochastic propagation of excitation waves. We have evaluated the exponent of the power-law distribution for some system sizes. However, the precise evaluation of the exponent of the power-law distribution and the theoretical analysis are left to the future study. We have further performed numerical simulations of the coupled noisy FitzHugh-Nagumo equations with a feedback control term and showed that a nearly critical state can be realized by the feedback control.

[1] A. L. Hodgkin and A. F. Huxley, J. Physiol. **117**, 500 (1952).
[2] R. FitzHugh, Biophys. J. **1**, 445 (1961).
[3] J. Nagumo, S. Arimoto, and S. Yoshizawa, Proc. IRE. **50**, 2061 (1962).
[4] S. Rajasekar and M. Lakshmanan, Physica D **32**, 146 (1988).
[5] K. Pyragas, V. Novicenko, and P. A. Tass, Biol. Cyberne. **107**, 669 (2013).
[6] H. Sakaguchi and K. Yamasaki, Phys. Rev. E **108**, 014207 (2023).
[7] B. Lindner, J. Varcia-Ojalvo, A. Neiman, and L. Schimansky-Geier, Phys. Rep. **392**, 321 (2004).
[8] F. Sagués, J. M. Sancho, and J. Garcia-Ojalvo, Rev. Mod. Phys. **79**, 829 (2007).
[9] A. S. Pikovsky and J. Kurths, Phys. Rev. Lett. **78**, 775 (1997).
[10] L. Gammaitoni, P. Hänggi, P. Jung, and F. Marchesoni, Rev. Mod. Phys. **70**, 223 (1998).
[11] H. Sakaguchi, S. Shinomoto, and Y. Kuramoto, Prog. Theor. Phys. **79**, 600 (1988).
[12] R. Rodriguez and H. C. Tuckwell, Phys. Rev. E **54**, 5585 (1996).
[13] A. Neiman, V. S. Anishchenko, and J. Kurths, J. Phys. A **28**, 2471 (1995).
[14] A. Neiman, L. Schimansky-Geier, A. Cornell-Bell, and F. Moss, Phys. Rev. Lett. **83**, 4896 (1999).
[15] P. Jung and G. Mayer-Kress, Chaos **5**, 458 (1995).
[16] S. Kádár, J. Wang, and K. Showalter, Nature (London) **391**, 770 (1998).
[17] J. García-Ojalvo and I. Schimansky-Geier, Europhys. Lett. **47**, 298 (1999).
[18] J. Wang, S. Kádár, P. Jung, and K. Showalter, Phys. Rev. Lett. **82**, 855 (1999).
[19] J. Beggs and D. Plenz, J. Neurosci. **23**, 11167 (2003).
[20] W. Freeman, L. Rogers, M. Holmes, and D. Silbergeld, J. Neurosci. Methods **95**, 111 (2000).
[21] P. Bak, C. Tang, and K. Wiesenfeld, Phys. Rev. Lett. **59**, 381 (1987).
[22] C. Meisel and T. Gross, Phys. Rev. E **80**, 061917 (2009).
[23] D. Millman, S. Mihalas, A. Kirkwood, and E. Niebur, Nat. Phys. **6**, 801 (2010).
[24] M. A. Muñoz, Rev. Mod. Phys. **90**, 031001 (2018).
[25] S. V. Buldyrev, A.-L. Barabasi, F. Caserta, S. Havlin, H. E. Stanley, and T. Vicsek, Phys. Rev. A **45**, R8313 (1992).
[26] H. Sakaguchi, Phys. Rev. E **82**, 032101 (2010); H. Sakaguchi and Y. Zhao, J. Phys. Soc. Jpn. **88**, 024006 (2019).
[27] Z. Olami, H. J. S. Feder, and K. Christensen, Phys. Rev. Lett. **68**, 1244 (1992).
[28] E. Domany and W. Kinzel, Phys. Rev. Lett. **53**, 311 (1984).
[29] R. Stoop and F. Gomez, Phys. Rev. Lett. **117**, 038102 (2016).
[30] L. Kuśmierz, S. Ogawa, and T. Toyoizumi, Phys. Rev. Lett. **125**, 028101 (2020).